RESEARCH ARTICLE

Distinct neuroanatomic subtypes in antipsychotic-treated patients with schizophrenia classified by the predefined classification in a never-treated sample

Qiannan Zhao[1,2,3,#], Jiao Li[4,5,#], Yuan Xiao[1,2,3,#], Hengyi Cao[1,6,7], Xiao Wang[4,5], Wenjing Zhang[1,2,3], Siyi Li[1,2,3], Wei Liao[4,5], Qiyong Gong[1,2,3,*] and Su Lui[1,2,3,*]

[1]Huaxi MR Research Center (HMRRC), Department of Radiology, West China Hospital of Sichuan University, Chengdu 610041, China
[2]Research Unit of Psychoradiology, Chinese Academy of Medical Sciences, Chengdu 610041, China
[3]Functional and Molecular Imaging Key Laboratory of Sichuan Province, West China Hospital of Sichuan University, Chengdu 610041, China
[4]The Clinical Hospital of Chengdu Brain Science Institute, School of Life Science and Technology, University of Electronic Science and Technology of China, Chengdu 610054, China
[5]MOE Key Lab for Neuroinformation, High-Field Magnetic Resonance Brain Imaging Key Laboratory of Sichuan Province, University of Electronic Science and Technology of China, Chengdu 610054, China
[6]Center for Psychiatric Neuroscience, Feinstein Institute for Medical Research, Manhasset, NY 11030, United States
[7]Division of Psychiatry Research, Zucker Hillside Hospital, Glen Oaks, NY 11004, United States

*Correspondence: Su Lui, lusuwcums@tom.com; Qiyong Gong, qiyonggong@hmrrc.org.cn
#Contributed equally to this article (joint first authors).

Abstract

Background: Distinct neuroanatomic subtypes have been identified in never-treated patients with schizophrenia based on cerebral structural abnormalities, but whether antipsychotic-treated patients would be stratified under the guidance of such previously formed classification remains unclear.
Objective: The present study aimed to investigate alterations of brain structures in antipsychotic-treated patients with schizophrenia based on a predefined morphological classification and their relationships with cognitive performance.

Methods: Cortical thickness, surface area, and subcortical volume were extracted from 147 antipsychotic-treated patients with schizophrenia using structural magnetic resonance imaging for classification. The Brief Assessment of Cognition in Schizophrenia (BACS) and Positive and Negative Syndrome Scale (PANSS) were used to assess cognition and symptoms.

Results: Antipsychotic-treated patients were categorized into three subtypes with distinct patterns of brain morphological alterations. Subtypes 1 and 2 were characterized by widespread deficits in cortical thickness but relatively limited deficits in surface area. In contrast, subtype 3 demonstrated cortical thickening mainly in parietal-occipital regions and widespread deficits in surface area. All three subgroups demonstrated cognitive deficits compared with healthy controls. Significant associations between neuroanatomic and cognitive abnormalities were only observed in subtype 1, where cortical thinning in the left lingual gyrus was conversely related to symbol coding performance.

Conclusions: Similar to drug-naïve patients, neuroanatomic heterogeneity exists in antipsychotic-treated patients, with disparate associations with cognition. These findings promote our understanding of relationships between neuroanatomic abnormalities and cognitive performance in the context of heterogeneity. Moreover, these results suggest that neurobiological heterogeneity needs to be considered in cognitive research in schizophrenia.

Key words: schizophrenia; neuroanatomic heterogeneity; psychoradiology; cognitive function; antipsychotic medication

Introduction

Schizophrenia is a severe psychiatric disorder with heterogeneity, based on the current nosology, where the diagnosis relies heavily on symptom-based criteria (Owen *et al*., 2016). Patients under the diagnosis of schizophrenia might be heterogeneous both clinically and biologically (Owen *et al*., 2016). Thus, heterogeneity is a critical consideration in searching for reliable biomarkers for the diagnosis, treatment, and prognosis of this disorder. This is particularly important in case-control designs, in which the diagnosed population was usually treated as a whole, ignoring the variability between patients. Studies focusing on individual variability of brain structures have revealed that schizophrenia was associated with more significant cortical and subcortical variability than healthy controls (Brugger and Howes, 2017; Alnaes *et al*., 2019). These findings provide evidence to support the notion that the identification of subtypes based on brain morphological features could potentially penetrate the neurobiological heterogeneity of schizophrenia (Voineskos *et al*., 2020). Stratifying schizophrenia into more homogeneous subgroups might be a workable approach to decompose such heterogeneity toward the intention of precision medicine in psychiatry (Jameson and Longo, 2015).

Recent studies have stratified patients with schizophrenia based on their neuroanatomic features and identified multiple subtypes with different degrees of abnormalities (Gupta *et al*., 2017; Chand *et al*., 2020; Pan *et al*., 2020). The main problem for such studies is that the application and generalization of such identified patient subsets remain to be clarified. Explaination is required as to whether the observed distinct neuroanatomic patterns rather than the subtyping algorithms in a specific sample could be used to guide classification in other patient cohorts. It is of importance to solve this problem, which will provide comparisons between patient populations with different demographics, medications, and psychopathological profiles and a better understanding of illness-related and medication-related phenotypes in the context of heterogeneity.

In our previous work (Xiao *et al*., 2021), three neuroanatomic subtypes were identified in 163 never-treated patients with schizophrenia using cortical and subcortical features based on a density peak-based clustering (DPC) algorithm, which is superior to approaches such as *K*-means or *K*-medoids by better detecting nonspheric clusters and automatically identifying cluster numbers. In the never-treated sample, subtype 1 was characterized by cortical deficits in the cortical-thalamic-cortical circuits and cortical thickening in the left rostral cingulate gyrus, while subtypes 2 and 3 showed near-normal cortical and subcortical measures relative to controls. The clustering algorithm applied in the never-treated sample was successfully used in a multisite cohort with mid-term illness, indicating the robustness of the three-subtype solution. This identification of subtypes in a never-treated sample with schizophrenia provides heterogeneous neuroanatomic profiles without the influence of medication. Antipsychotics have been reported to relate to neuroanatomic changes such as cortical thinning and increases and decreases of volumes in the basal ganglia (van Haren *et al*., 2011; Haijma *et al*., 2013; Jorgensen *et al*., 2016). Our question is, what would the neuroanatomic patterns be if a cohort of antipsychotic-treated patients could be classified by the previously formed subtypes in the never-treated patients? Moreover, cognitive deficits in multiple domains have been associated with different brain structural abnormalities (Kelly *et al*., 2019). Another question is, what would the associations with cognitive function be for

neuroanatomic profiles in patients that received medication in the context of heterogeneity?

In the present study, we aimed to investigate (i) whether a cohort of patients with schizophrenia that received antipsychotic medication would be classified into subtypes based on a predefined classification in a never-treated sample, and (ii) what the neuroanatomic patterns and their associations with cognition would be in the treated sample. It is worth noting that the antipsychotic-treated sample was recruited from the same site with the cohort of never-treated patients used in our previous work (Xiao *et al.*, 2021). All participants from these two samples were scanned by a magnetic resonance scanner with the same parameters and rated by the same trained raters for behavioral assessments. The consistency of research settings helps to eliminate potential confounding factors across samples. Here, the stratification was performed based on structural individual-subtype similarity, representing the morphological similarity between each individual in the present study and the three previously generated subtypes. According to previous studies (Finn *et al.*, 2015; Shen *et al.*, 2017; Cai *et al.*, 2021), similarity, measured by Pearson's correlation coefficient, has been successfully used for identifying individuals based on functional connectome. In this work, we hypothesized that (i) antipsychotic-treated patients with schizophrenia would be stratified into distinct neuroanatomic patterns based on the predefined morphological classification, and (ii) three subgroups of antipsychotic-treated patients with schizophrenia would have different cognitive patterns and diverse relationships between cognitive performances and cerebral morphologies.

Materials and Methods

Participants

This study included 147 antipsychotic-treated patients with schizophrenia and 147 age- and sex-matched healthy participants. Patients with schizophrenia were diagnosed using the Structured Clinical Interview for DSM-IV Axis I Disorders (SCID). Clinical symptoms were assessed using the Positive and Negative Syndrome Scale (PANSS) (Kay *et al.*, 1987), and the Global Assessment of Functioning Scale (Hall, 1995) was also evaluated. The average daily dose of antipsychotics was transformed into chlorpromazine equivalent dose (mg/day) based on an international consensus study (Gardner *et al.*, 2010). The nonpatient edition of SCID was completed to confirm the absence of lifetime psychiatric disorder for healthy participants recruited by advertisement. Healthy individuals with a first-degree relative with major psychotic disorders were excluded. Exclusive criteria for all participants were as follows: (i) head injury history; (ii) history of intracranial tumor, hematoma, inflammation, or other physical diseases; (iii) alcohol or drug abuse; (iv) age below 16 or over 70 years; and (v) individuals

with magnetic resonance imaging (MRI) contraindication. The study protocol was approved by the local medical research ethics committee, and written informed consent was provided by all participants.
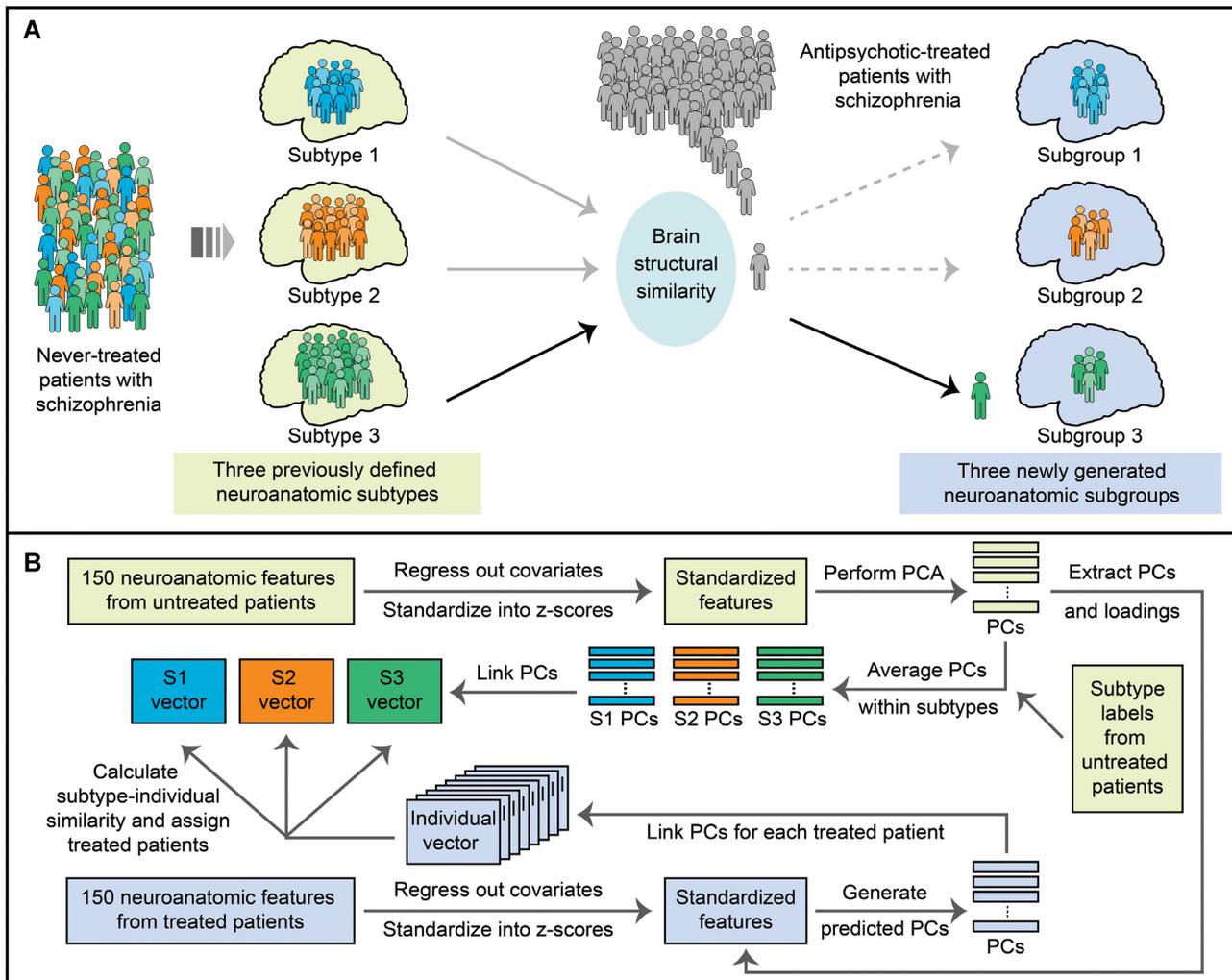
For the 163 never-treated patients with schizophrenia employed in defining original neuroanatomic subtypes, detailed descriptions can be found in our previous publication (Xiao *et al.*, 2021). It is worth noting that patients in the antipsychotic-treated sample were not overlapped with those in the never-treated sample.

Structural imaging acquisition and preprocessing

We acquired 3D T1-weighted images on a 3.0 Tesla General Electric Signa EXCITE magnetic resonance scanner from all participants. The parameters of magnetic resonance acquisition and quality inspection procedure were displayed in the Supplementary Methods. Structural imaging data of all participants were processed using recon-all stream by FreeSurfer software version 6.0 (https://surfer.nmr.mgh.harvard.edu). Consistent with our previous clustering in never-treated patients, we extracted a total of 150 neuroanatomic features for subtyping in antipsychotic-treated patients, including thickness and surface area of 68 cortical regions based on Desikan–Killiany atlas (Desikan *et al.*, 2006) and volume of 14 subcortical structures (bilateral thalamus, caudate nucleus, putamen, nucleus accumbens, hippocampus, and amygdala). The volume of 68 cortical regions and global brain measures, such as cortical gray matter volume (GMV), cerebral white matter volume (WMV), subcortical GMV, total GMV, total brain volume (TBV), and estimated total intracranial volume (ICV) was also obtained for statistical inferences.

Cognitive function assessment

The Brief Assessment of Cognition in Schizophrenia (BACS) (Keefe *et al.*, 2004) has been widely used to measure cognition for patients with schizophrenia. It contains six cognitive domains, including verbal memory (measured by list learning subtest), working memory (measured by digit sequencing subtest), motor speed (measured by token motor subtest), verbal fluency (measured by category instances subtest and controlled oral word association subtest), attention and speed of information processing (measured by symbol coding subtest), and executive functioning (measured by Tower of London subtest). An authorized and certified Chinese version of BACS was used to assess the cognitive performance of patients and healthy controls. Validity and high test–retest reliability have been confirmed in the Chinese version of BACS (Wang *et al.*, 2016). Since bias might be caused by directly applying western norms of BACS to the Mandarin-speaking population (Wang *et al.*, 2017), we reported original scores of the BACS instead of transforming them into z-scores.

Figure 1: Scheme of stratification of antipsychotic-treated patients with schizophrenia based on previously defined neuroanatomic subtypes. (A) Three neuroanatomic subtypes were previously identified in never-treated patients with schizophrenia. In the present work, each patient from the antipsychotic-treated sample was classified into three subgroups based on their brain structural similarity to the three subtypes. (B) Brain structural similarity, measured by Pearson's correlation coefficient, was calculated for patient assignment in the antipsychotic-treated sample. First, we extracted standardized neuroanatomic features in never-treated patients after regressing out corresponding covariates and z-scoring and performed a PCA on them. PCs and loadings from the never-treated sample were applied to standardized neuroanatomic features of treated patients, producing predicted PCs for each participant. Second, we averaged PCs of never-treated patients per subtype, and three subtypes of PCs were generated. Third, we linked averaged PCs in each subtype by descending order of their contributions, which was also done for the PCs of each patient from the treated sample. Thus, three subtype vectors from the never-treated sample, and a group of individual vectors from the treated sample, were generated for subsequent similarity calculations. Fourth, we calculated subtype-individual similarity, measured by Pearson's correlation coefficients, between three subtype vectors and each individual vector. Every treated patient was assigned into one of the three subtypes according to the corresponding largest similarity, and three subgroups of treated patients were finally formed. S1–S3, Subtypes 1–3 of never-treated patients with schizophrenia.

Subtyping based on neuroanatomic similarity

Each patient in the antipsychotic-treated sample was classified based on previously identified subtypes in never-treated patients through individual-subtype similarity of brain morphology (Fig. 1). In our previous work (Xiao *et al.*, 2021), 163 never-treated patients with schizophrenia were clustered into three distinct neuroanatomic subtypes using a DPC algorithm. The rationale for the present study is to explore a more generalizable approach for subtyping participants based on previously formed subtypes rather than to be restricted by study-specific algorithms. Thus, we did not classify

antipsychotic-treated patients with DPC-based centers generated in the never-treated sample but used brain structural similarity in the subtyping process, independent of previously used algorithms. A total of 150 neuroanatomic features composed of cortical and subcortical measures were adopted for subtyping. First, variance related to age and sex was removed before subtyping for 147 antipsychotic-treated patients to be stratified in this study and 163 never-treated patients applied in our previous work (Xiao *et al.*, 2021). It is worth noting that variance related to ICV was additionally removed for surface area and volume features. Features were then

standardized into z-scores after removing potential confounding variance. A principal component analysis (PCA) was performed among 150 neuroanatomic features in never-treated patients, where principal components (PCs) and corresponding loadings were subsequently applied in the antipsychotic-treated sample. Neuroanatomic PCs in never-treated patients were averaged within three predefined subtypes; thus, three groups of averaged PCs were generated. Each group of averaged PCs was ranked in descending order by their contributions, and three subtype vectors were formed. For each patient in the antipsychotic-treated sample, generated individual PCs were also linked as individual vectors. We then calculated the similarity, quantified by Pearson correlation coefficient, between individual vectors and each of the three subtype vectors. Every participant in the antipsychotic-treated sample was classified based on the subtype that achieved the largest individual-subtype similarity. Finally, antipsychotic-treated patients were classified into three groups according to the three predefined neuroanatomic subtypes in never-treated patients. We demonstrated similarity distributions for the antipsychotic-treated sample to better display the subtyping process (Supplementary Figs S1 and S2). As a secondary subtyping analysis, variance related to antipsychotic dose was additionally removed before subtyping (see Supplementary Materials).

Statistical analysis

Between-group comparisons were conducted among three identified subtypes of antipsychotic-treated patients and healthy controls. Antipsychotic types were classified into three categories: treatment with first-generation antipsychotics, treatment with second-generation antipsychotics, and treatment with both types. Distributions of sex, antipsychotic type, and the status of receiving clozapine treatment or not were tested using Pearson's chi-square test. Between-group differences in age, education level, illness duration, age at illness onset, the daily dose of antipsychotics, and psychopathological symptoms were tested with one-way analysis of variance (ANOVA). One-way analysis of covariance (ANCOVA) was employed to assess between-group differences in neuroanatomic and cognitive features. Specifically, age and sex were treated as covariates for cortical thickness, and ICV was the additional covariate for other neuroanatomic features. In terms of cognitive scores, covariates were composed of age, sex, and education level. Tukey's HSD tests were used as pairwise comparisons for features shown to be significantly different in main tests of ANOVA or ANCOVA. To explore relationships between cognitive function and cerebral structures in each subgroup, correlation analyses were performed between brain structures and BACS scores with the prior removal of corresponding covariates. False discovery rate (FDR) correction was separately performed for multiple comparisons in each kind of neuroanatomic features, BACS and PANSS scores. The

FDR correction was also used while multiple correlations were performed at the same time. Data were analyzed with R v.4.0.2, and the statistically significant level was set at two-tailed $P < 0.05$.

Results

Demographical, clinical, and cognitive comparisons

Based on neuroanatomic similarity to three predefined subtypes in a never-treated sample, three subtypes of antipsychotic-treated patients were identified, including 55 patients (37.4%) in subtype 1, 34 patients (23.1%) in subtype 2, and 58 patients (39.5%) in subtype 3.

Demographical, clinical, and cognitive comparisons among three subgroups of patients and (or) healthy controls are displayed in Table 1. Subtype 2 had greater age at illness onset than both subtypes 1 and 3 ($F = 4.86$, $P = 0.009$). Participants in different groups did not show any significant differences in age, sex, or education level. Three subtypes of patients did not differ in illness duration, antipsychotic dose, antipsychotic type, symptoms, or general psychopathological function.

Concerning cognitive profiles, three subtypes displayed cognitive deficits relative to healthy controls, involving almost all domains except the domain of verbal fluency, but no significant between-subtype differences were observed.

Neuroanatomic comparisons

Three subtypes of antipsychotic-treated patients with schizophrenia demonstrated distinct neuroanatomic patterns (Figs 2–4), different from those revealed by the never-treated sample. In the antipsychotic-treated sample, neuroanatomic patterns for subtypes identified by the secondary subtyping analysis were similar to those primary findings (see Supplementary Figs S3–S5).

Cortical measures
The abnormal patterns in cortical thickness and surface area for three subtypes were in contrast (Figs 2 and 3). Subtypes 1 and 2 had severe and widespread thickness deficits involving the most cortical regions, while subtype 3 showed thicker cortices, mainly in parietal-occipital regions and the limbic system. Subtype 1 displayed surface area deficits in regions such as the prefrontal cortex and middle temporal gyrus, and subtype 2 had more severe and widespread deficits than subtype 1. In contrast, subtype 3 displayed the most widespread surface area deficits involving almost all neocortical regions. For regional cortical volume, all of the three subtypes displayed reductions relative to controls. However, the between-subtype differences in cortical volumes were subtle, which even disappeared in comparing secondary subtyping findings (Fig. S4 in Supplementary Materials).

Table 1: Demographical and psychopathological comparisons between three subtypes of antipsychotic-treated patients with schizophrenia and healthy controls

Measure	Group				Comparison	
	Subtype 1 (N = 55)	Subtype 2 (N = 34)	Subtype 3 (N = 58)	HC (N = 147)	F/χ^2	P/P_{FDR}
Age (years, M ± SD)	46.11 ± 7.45	47.76 ± 6.67	46.78 ± 7.53	45.86 ± 9.99	0.50	0.680
Sex (female: N/%)	20 (36.36%)	17 (50.00%)	18 (31.03%)	55 (37.42%)	3.33	0.343
Education level (years, M ± SD)	9.6 ± 3.03	9.39 ± 2.06	10.11 ± 3.69	10.13 ± 3.99	0.58	0.626
Illness duration (years, M ± SD)	20.81 ± 9.63	17.48 ± 8.71	20.66 ± 8.52		1.66	0.193
Age at onset (years, M ± SD)	25.19 ± 8.58	30.27 ± 8.13	25.89 ± 6.55		4.86	0.009[d,e]
Antipsychotic dose (mg/day, M ± SD)	595.83 ± 333.52	480.80 ± 353.13	520.89 ± 199.26		1.72	0.182
Antipsychotic type (FGA/SGA/both: N)	3/38/12	6/25/2	5/36/12		7.08	0.132
Clozapine-treated (treated/untreated: N)	32/21	17/16	27/26		1.13	0.569
PANSS (M ± SD)						
Positive scale	10.25 ± 4.10	11.19 ± 5.04	10.00 ± 4.39		0.75	0.793
Negative scale	17.27 ± 6.15	15.75 ± 5.00	16.14 ± 5.43		0.88	0.793
General scale	25.16 ± 5.45	26.50 ± 5.42	25.77 ± 6.42		0.52	0.793
Total score	52.69 ± 13.43	53.44 ± 13.44	51.91 ± 13.65		0.13	0.875
GAF (M ± SD)	58.27 ± 14.81	56.84 ± 12.82	59.36 ± 15.88		0.29	0.749
BACS (M ± SD)						
Verbal memory	27.39 ± 10.63	24.41 ± 10.55	27.04 ± 9.83	32.22 ± 10.91	4.72	0.004[b,c]
Working memory	14.66 ± 5.06	14.14 ± 5.12	16.02 ± 5.20	18.63 ± 5.78	8.39	<0.001[a,b,c]
Motor speed	53.76 ± 15.34	52.14 ± 12.70	55.19 ± 14.61	66.08 ± 15.34	12.52	<0.001[a,b,c]
Verbal fluency	20.85 ± 7.34	19.34 ± 6.16	22.02 ± 7.41	22.63 ± 7.16	1.74	0.161
Attention and speed of information processing	27.32 ± 12.81	24.59 ± 13.60	29.53 ± 13.59	37.67 ± 13.13	15.86	<0.001[a,b,c]
Executive functioning	13.85 ± 5.34	12.69 ± 6.10	16.11 ± 3.67	17.49 ± 2.32	10.07	<0.001[a,b]
General function (composite score)	26.30 ± 7.30	24.55 ± 6.75	27.65 ± 6.50	32.46 ± 6.65	18.15	<0.001[a,b,c]

FGA, first-generation antipsychotics; GAF, Global Assessment of Functioning Scale; HC, healthy control subjects; M, mean value; P_{FDR}, P-value adjusted with FDR; SD, standard deviation; SGA, second-generation antipsychotics. Antipsychotic dose represents average daily dose of antipsychotics that patients received, which was transformed into chlorpromazine equivalent. Antipsychotic types were classified into three categories, including treatment with first-generation antipsychotics, treatment with second-generation antipsychotics, and treatment with both types. Distributions of sex, antipsychotic type, and the status that received clozapine-treatment or not were tested using chi-square tests; Cognitive between-group differences were tested using one-way ANCOVA. All other between-group comparisons were performed under a one-way ANOVA test. Tukey's HSD test was performed as post hoc analyses after one-way ANOVA or ANCOVA. FDR correction was used for P-values of PANSS scores.

[a]Patients in subtype 1 are significantly smaller than healthy controls;
[b]Patients in subtype 2 are significantly smaller than healthy controls;
[c]Patients in subtype 3 are significantly smaller than healthy controls;
[d]Patients in subtype 1 are significantly smaller than those in subtype 2;
[e]Patients in subtype 2 are significantly greater than those in subtype 3.

A Cortical thickness

B Cortical surface area

C Cortical volume
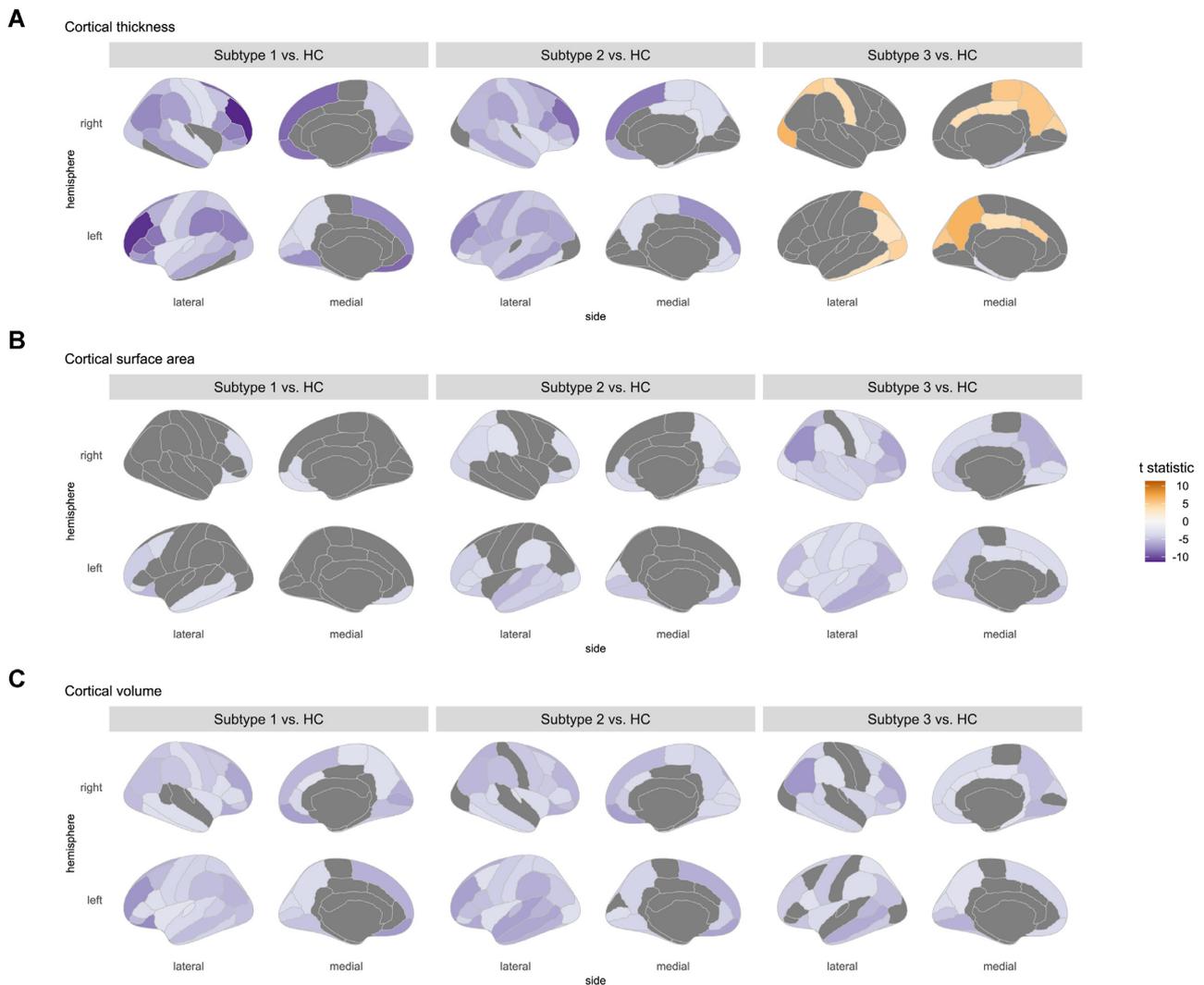
Figure 2: Cortical statistic maps for comparisons between each of the three subgroups of antipsychotictreated patients with schizophrenia and healthy controls. Cortical features including (A) cortical thickness, (B) cortical surface area, and (C) cortical volume were used in between-group comparisons, where age and sex were treated as covariates for thickness, and ICV was as an additional covariate for surface area and volume. Only regions that survived in multiple comparison corrections were demonstrated and scaled by *t* statistic.

Subcortical measures

Regarding subcortical abnormalities (see Fig. 4), all three subtypes showed decreased volumes in the bilateral thalamus and the left nucleus accumbens. Except for these common abnormalities, subtype 1 displayed reductions in bilateral caudate and the right nucleus accumbens and increases in the right pallidum, which is the only finding of greater subcortical volume than controls revealed by three subtypes. Subtype 2 showed additional reductions in the left putamen. Subtype 3 had additional reductions in the bilateral hippocampus, amygdala, and the right nucleus accumbens, displaying more severe subcortical deficits.

Global brain measures

Three subtypes of antipsychotic-treated patients showed reductions in cortical GMV, total GMV, cerebral WMV, and TBV, and subtypes 2 and 3 additionally had reductions in subcortical GMV. However, no significant between-subtype differences in global brain volumes were found (Table S1 in Supplementary Materials).

Differences between subtypes identified in two samples

Compared with findings revealed by our previous work (Xiao *et al.*, 2021), three subtypes of antipsychotic-treated patients displayed different patterns of neuroanatomic abnormalities from those in the never-treated patients. Specifically, significant cortical and subcortical abnormalities in subtypes 2 and 3 were only observed in antipsychotic-treated patients instead of the never-treated sample. Regarding subtype 1, in which both samples displayed neuroanatomic alterations, antipsychotic-treated patients showed some overlaps in cortical surface area and thalamic deficits but more severe reductions in cortical thickness relative to never-treated patients.

A Cortical thickness

B Cortical surface area
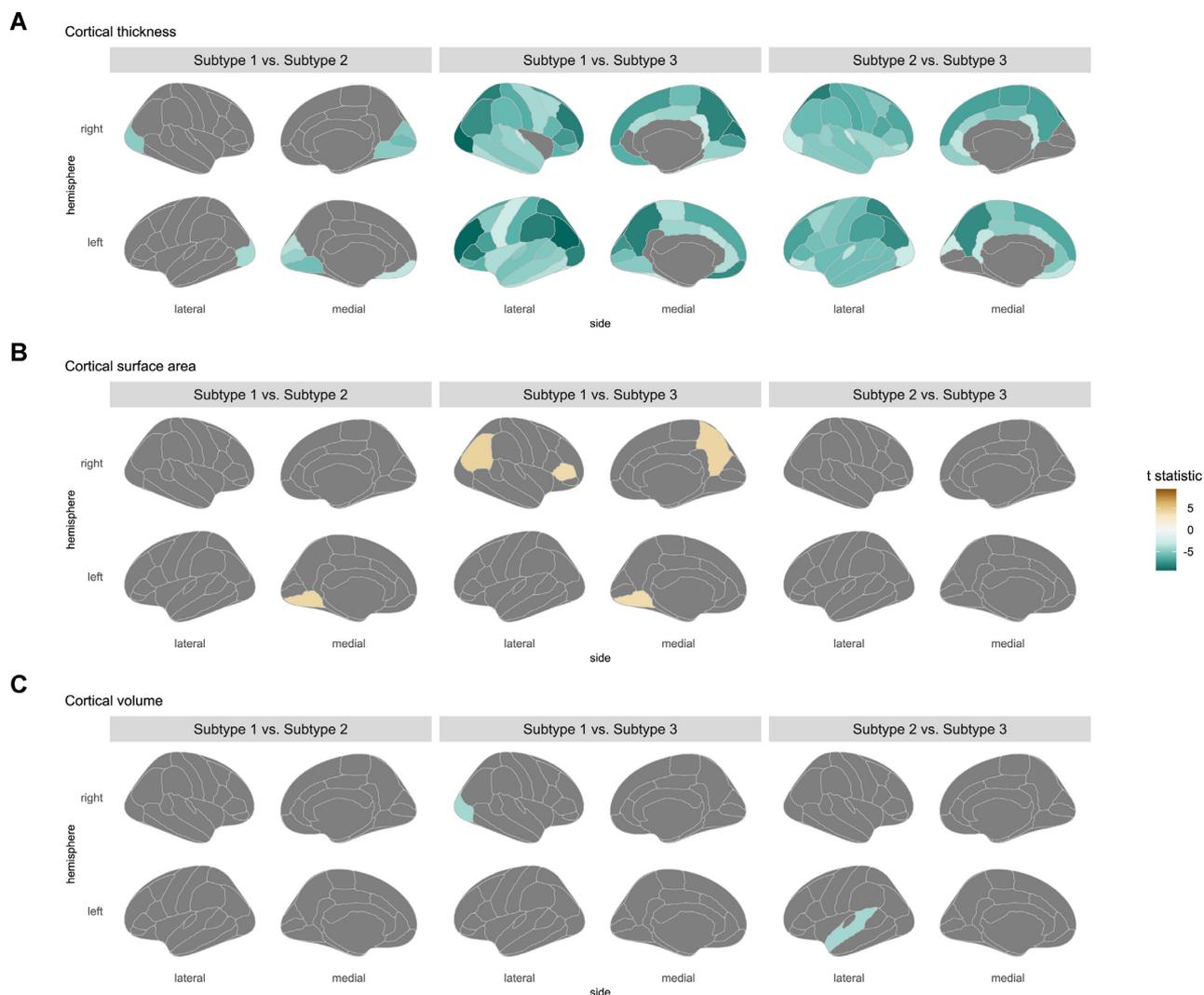
C Cortical volume

Figure 3: Cortical statistic maps for comparisons between three subgroups of antipsychotic-treated patients. Cortical features including (A) cortical thickness, (B) cortical surface area, and (C) cortical volume were employed in between-group comparisons, where age and sex were treated as covariates for thickness, and ICV was as an additional covariate for surface area and volume. Only regions that survived in multiple comparison corrections are demonstrated and scaled by t statistic.

Correlation between cognitive or clinical profiles and neuroanatomic features

Three subtypes of antipsychotic-treated patients with schizophrenia demonstrated disparate profiles in terms of associations with cognitive function or clinical profiles.

Significant correlations with cognitive scores were only observed in subtype 1 (Fig. 5). For regional brain measures, a significant correlation was found between cortical thinning in the left lingual gyrus and cognitive score of symbol coding ($r = -0.57$, $P_{FDR} = 0.012$) in subtype 1. Concerning global brain volumes, significant correlations were found between general cognitive function and decreased cerebral WMV ($r = 0.42$, $P_{FDR} = 0.012$), total GMV ($r = 0.42$, $P_{FDR} = 0.012$), and TBV ($r = 0.45$, $P_{FDR} = 0.012$) in subtype 1.

In subtype 1, right middle temporal volume was significantly correlated with age at onset ($r = 0.50$,

$P_{FDR} = 0.009$), which were not found in subtypes 2 or 3 (see Supplementary Fig. S6). No significant correlations between neuroanatomic features and antipsychotic dose or illness duration were found in any subtypes of antipsychotic-treated patients.

Discussion

We classified antipsychotic-treated patients with schizophrenia into three subtypes based on their neuroanatomic similarity with three predefined subtypes of a never-treated schizophrenia sample. Three neuroanatomic subtypes of antipsychotic-treated patients displayed distinct patterns of morphological abnormalities, which were different from the patterns revealed by the never-treated sample. Compared with healthy controls, subtypes 1 and 2 were characterized by widespread deficits in cortical thickness but limited deficits in

Subcortical volume
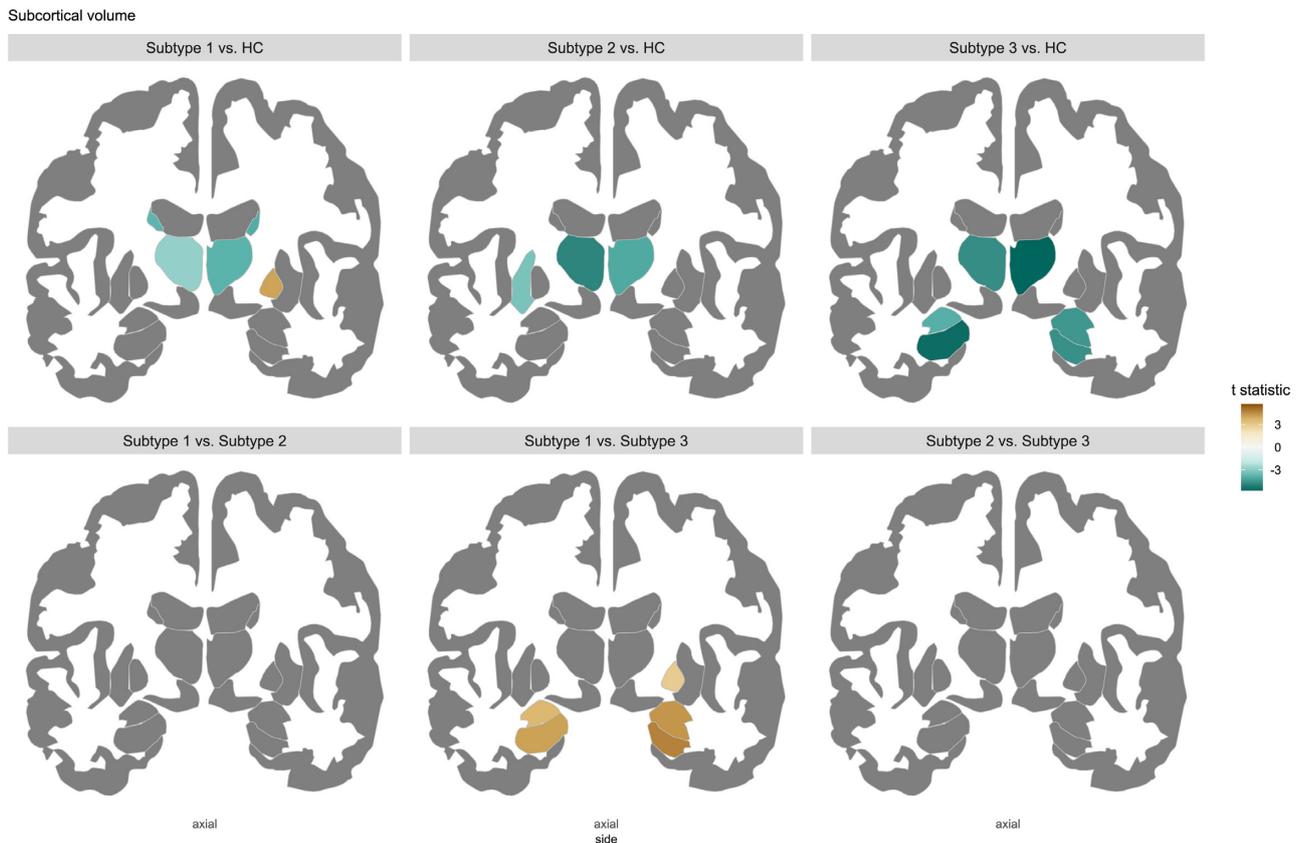
Figure 4: Subcortical statistic maps for comparisons among three subgroups of antipsychotic-treated patients and healthy controls. In subcortical volume comparison, age, sex, and ICV were treated as covariates. Only regions that survived in multiple comparison corrections are demonstrated and scaled by *t* statistic. Comparison results in the nucleus accumbens cannot be demonstrated in this 2D figure but described in the Results.

cortical surface area. In contrast, subtype 3 displayed cortical thickening affecting limited regions but widespread deficits in surface area. Significant correlations between neuroanatomic measures and cognitive function were only found in subtype 1. Specifically, cortical thinning in the left lingual gyrus was conversely associated with symbol coding scores, and decreased cerebral WMV, total GMV, and TBV were correlated with general cognitive function.

To our knowledge, our research is the first study to stratify antipsychotic-treated patients with schizophrenia based on the similarity of brain structures with the predefined neuroanatomic subtypes of a never-treated sample. The three generated subtypes of antipsychotic-treated patients displayed various patterns of neuroanatomic abnormalities, different from those revealed by the never-treated sample. It is worth noting that such across-sample differences in neuroanatomic patterns were not driven by potential confounding factors. All participants from the two cohorts were from a single site, scanned with the same scanner, with no comorbidities or substance use history, allowing us to better characterize neuroanatomic heterogeneity in different illness stages and medication conditions. The successful subtyping based on previously formed neuroanatomic subtypes indicates a workable way to apply and generalize

predefined data-driven subtypes. Our attempt moves forward toward the notion that the translational impact of subtyping individuals with psychiatry into subtypes will ultimately depend on their utility (Voineskos *et al.*, 2020).

A somewhat unexpected finding is that subtype 3 of antipsychotic-treated patients with schizophrenia displayed cortical thickening in the parietal-occipital regions and the limbic system. Cortical thinning has been frequently observed in schizophrenia no matter whether patients received antipsychotics or not (Rimol *et al.*, 2012; Xiao *et al.*, 2015; Zhang *et al.*, 2015; van Erp *et al.*, 2018). In contrast, cortical thickening is a less observed phenomenon, reported in untreated patients or individuals at-risk mental state with affected parietal-occipital areas. (Xiao *et al.*, 2015; Zhang *et al.*, 2015; Suzuki *et al.*, 2020). This evidence from individuals without antipsychotic medications indicates that our finding in subtype 3 might be an illness-related characteristic rather than the results of antipsychotic treatment. The result that no significant correlations between neuroanatomic features and antipsychotic dose found in any of the three subtypes also supports this notion. However, the influence of antipsychotics on the thicker posterior cortices cannot be eliminated entirely. It is worth noting that the effects of antipsychotic treatment on brain structures might be complicated. Multiple aspects in
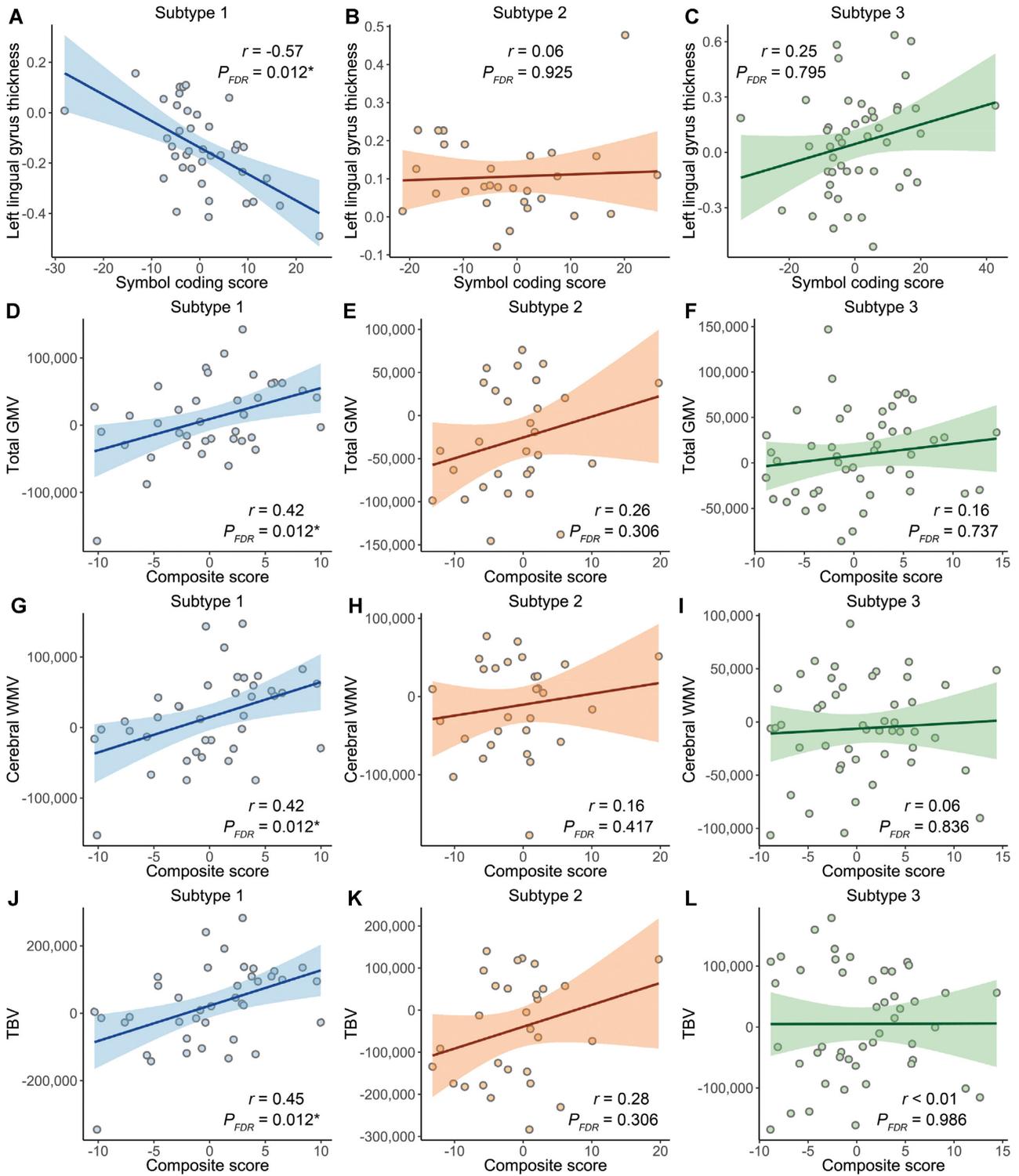
Figure 5: Correlation between cognitive function and neuroanatomic features in each of the three subtypes of antipsychotic-treated patients with schizophrenia. Correlation analyses were conducted between cognitive scores and neuroanatomic features in each of the three identified subtypes of antipsychotic-treated patients with schizophrenia. We employed cortical thickness, cortical surface area, cortical and subcortical volumes, and global brain volumes for analysis. Covariates for cognitive and neuroanatomic features were removed before analyzing. Specifically, age and sex were treated as covariates for cortical thickness, and ICV was the additional covariate for other neuroanatomic features. For cognitive scores, age, sex, and education level were treated as covariates. FDR-corrected P-values smaller than 0.05/3 were recognized as significant and marked with asterisks because multiple correlation analyses were performed in three subtypes. Only features involved in significant correlations in any of the three subtypes were displayed in this figure. P_{FDR}, FDR-corrected P-value; r, Pearson's correlation coefficient.

antipsychotic treatment, such as current dose (Fusar-Poli *et al.*, 2013), accumulative dose across the illness course (Vita *et al.*, 2015), treatment intensity that reflects antipsychotic dose in a specific interval (Andreasen *et al.*, 2013), and antipsychotic types (Vita *et al.*, 2015) might affect gray matter morphologies. The daily dose of antipsychotics representing treatment conditions around magnetic resonance scanning and the cross-sectional design in our work makes it challenging to clarify the relationship between cortical thickening and medication effects. Thus, research with a long-term follow-up that will establish relationships between neuroanatomic features and effects of antipsychotic treatments in the context of heterogeneity is highly required.

An interesting finding is that the thinning cortex in the left lingual gyrus is conversely associated with scores of symbol coding in subtype 1 of antipsychotic-treated patients with schizophrenia. Cortical thinning in the lingual gyrus has been reported in schizophrenia (Narr *et al.*, 2005; Oertel-Knochel *et al.*, 2013; Reavis *et al.*, 2017). As a part of the visual cortex, the lingual gyrus is located in the medial occipital lobe and associated with visual processing (Palejwala *et al.*, 2021). Activations in the lingual gyrus were found during the picture presentation task of functional MRI in patients with schizophrenia and healthy controls, indicating the function of visual perception of this area (Stephan-Otto *et al.*, 2016). In the symbol coding paradigm, participants are requested to match numbers to symbols within the allowed time, and this test performance is sensitive to cognitive deficits in a range of conditions (Jaeger, 2018), where patients with schizophrenia generally showed great effect sizes of deficits in this test (Dickinson *et al.*, 2007). The symbol coding paradigm measures a range of cognitive profiles, such as attention, processing speed, visuoperceptual function, motor speed, and working memory. The lingual gyrus was activated in healthy adults during the symbol coding test (Usui *et al.*, 2009). Functions involved in the symbol coding test, such as visual attention (Cornette *et al.*, 1998; Mechelli *et al.*, 2000) and working memory (Hanford *et al.*, 2019), are related to lingual gyrus in healthy populations or patients with schizophrenia. Based on the evidence of associations between lingual gyrus and symbol coding, we infer that more significant cortical thinning may be a biomarker of relative better performance in a subset of antipsychotic-treated patients. The microstructural cause of cortical thinning in the lingual gyrus in schizophrenia was unclear. Further work is needed to investigate pathophysiological mechanisms for this abnormality and its relationships with cognition to provide potential biomarkers for cognition-targeted treatment.

It is an expected finding that three subtypes of antipsychotic-treated patients demonstrated different patterns of neuroanatomic alterations from those revealed by the never-treated sample. Disparate profiles in antipsychotic medications or illness stages between the two samples might contribute to their differences in neuroanatomic patterns. In line with the notion that schizophrenia is a disorder with progressive brain changes (Olabi *et al.*, 2011; Kubota *et al.*, 2015), brain morphological alterations in the antipsychotic-treated sample at later illness stages were considerably more evident than those in the never-treated sample. Moreover, these across-sample differences in neuroanatomic patterns across samples align with the well-established roles of antipsychotics in cortical thinning and volumetric changes in the basal ganglia (van Haren *et al.*, 2011; Haijma *et al.*, 2013; Jorgensen *et al.*, 2016).

Several limitations of the present study need to be taken into account. First, as a cross-sectional design, the effects of antipsychotics and illness progression could hardly be evaluated when interpreting the heterogeneity of brain structures and their relationships with cognitive performance, although no between-group differences in antipsychotic dose and illness duration were revealed among three antipsychotic-treated subgroups. Thus, the stratification should be further employed in longitudinal research to explore such heterogeneity at different illness stages with comparable antipsychotic treatments. Second, as a structural MRI study, it is challenging to investigate potential neurobiological mechanisms of the distinct patterns of cerebral structural abnormalities among three subgroups of patients. Longitudinal research with antipsychotic use in animal models and analysis extending to genetics and molecular biology is required to characterize the neurobiological process for our findings. Last, we aimed to explore the neuroanatomic patterns if a cohort of antipsychotic-treated patients could be classified by the predefined subtypes in a never-treated sample. This rationale led us to use neuroanatomic similarity to perform subtyping rather than use data-driven approaches, limiting us to use any advanced clustering algorithms in the antipsychotic-treated sample. We used similarity, measured by Pearson's correlation coefficient, for patient subtyping. As a linear modeling approach, this method could hardly detect complex nonlinear relationships. Moreover, it tends to overfit data, although we performed dimensional reductions procedures (i.e. PCA) on neuroanatomic features before subtyping. Future work may seek to conduct patient subtyping using multivariate algorithms with larger sample size.

Conclusions

We stratified patients with schizophrenia into three subgroups based on cerebral structures. The three subtypes of patients demonstrated distinct patterns of neuroanatomic abnormalities but also disparate relationships between brain morphologies and cognitive functioning. These findings corroborate the existence of neurobiological heterogeneity in schizophrenia and suggest that heterogeneity is a critical consideration in understanding the complex associations between structural alterations and cognitive functioning.

Supplementary data

Supplementary data is available at *Psychoradiology* online.

Author contributions

Conflict of interest statement

Acknowledgements

References

Alnaes D, Kaufmann T, van der Meer D, *et al.*, Karolinska Schizophrenia Project C. (2019) Brain heterogeneity in schizophrenia and its association with polygenic risk. *JAMA Psychiatry* **76**:739–48.

Andreasen NC, Liu D, Ziebell S, *et al.* (2013) Relapse duration, treatment intensity, and brain tissue loss in schizophrenia: a prospective longitudinal MRI study. *Am J Psychiatry* **170**:609–15.

Brugger SP, Howes OD (2017) Heterogeneity and homogeneity of regional brain structure in schizophrenia: a meta-analysis. *JAMA Psychiatry* **74**:1104–11.

Cai B, Zhang G, Zhang A, *et al.* (2021) Functional connectome fingerprinting: identifying individuals and predicting cognitive functions via autoencoder. *Hum Brain Mapp* **42**:2691–705.

Chand GB, Dwyer DB, Erus G, *et al.* (2020) Two distinct neuroanatomical subtypes of schizophrenia revealed using machine learning. *Brain* **143**:1027–38.

Cornette L, Dupont P, Rosier A, *et al.* (1998) Human brain regions involved in direction discrimination. *J Neurophysiol* **79**:2749–65.

Desikan RS, Segonne F, Fischl B, *et al.* (2006) An automated labeling system for subdividing the human cerebral cortex on MRI scans into gyral based regions of interest. *Neuroimage* **31**:968–80.

Dickinson D, Ramsey ME, Gold JM (2007) Overlooking the obvious: a meta-analytic comparison of digit symbol coding tasks and other cognitive measures in schizophrenia. *Arch Gen Psychiatry* **64**:532–42.

Finn ES, Shen X, Scheinost D, *et al.* (2015) Functional connectome fingerprinting: identifying individuals using patterns of brain connectivity. *Nat Neurosci* **18**:1664–71.

Fusar-Poli P, Smieskova R, Kempton MJ, *et al.* (2013) Progressive brain changes in schizophrenia related to antipsychotic treatment? A meta-analysis of longitudinal MRI studies. *Neurosci Biobehav Rev* **37**:1680–91.

Gardner DM, Murphy AL, O'Donnell H, *et al.* (2010) International consensus study of antipsychotic dosing. *Am J Psychiatry* **167**:686–93.

Gupta CN, Castro E, Rachkonda S, *et al.* (2017) Biclustered independent component analysis for complex biomarker and subtype identification from structural magnetic resonance images in schizophrenia. *Front Psychiatry* **8**:179.

Haijma SV, Van Haren N, Cahn W, *et al.* (2013) Brain volumes in schizophrenia: a meta-analysis in over 18 000 subjects. *Schizophr Bull* **39**:1129–38.

Hall RC (1995) Global assessment of functioning. A modified scale. *Psychosomatics* **36**:267–75.

Hanford LC, Pinnock F, Hall GB, *et al.* (2019) Cortical thickness correlates of cognitive performance in cognitively-matched individuals with and without schizophrenia. *Brain Cogn* **132**:129–37.

Jaeger J (2018) Digit symbol substitution test: the case for sensitivity over specificity in neuropsychological testing. *J Clin Psychopharmacol* **38**:513–9.

Jameson JL, Longo DL (2015) Precision medicine–personalized, problematic, and promising. *N Engl J Med* **372**:2229–34.

Jorgensen KN, Nesvag R, Gunleiksrud S, *et al.* (2016) First- and second-generation antipsychotic drug treatment and subcortical brain morphology in schizophrenia. *Eur Arch Psychiatry Clin Neurosci* **266**:451–60.

Kay SR, Fiszbein A, Opler LA (1987) The positive and negative syndrome scale (PANSS) for schizophrenia. *Schizophr Bull* **13**:261–76.

Keefe RS, Goldberg TE, Harvey PD, *et al.* (2004) The Brief Assessment of Cognition in Schizophrenia: reliability, sensitivity, and comparison with a standard neurocognitive battery. *Schizophr Res* **68**:283–97.

Kelly S, Guimond S, Lyall A, *et al.* (2019) Neural correlates of cognitive deficits across developmental phases of schizophrenia. *Neurobiol Dis* **131**:104353.

Kubota M, van Haren NE, Haijma SV, *et al.* (2015) Association of IQ changes and progressive brain changes in patients with schizophrenia. *JAMA Psychiatry* **72**:803–12.

Mechelli A, Humphreys GW, Mayall K, *et al.* (2000) Differential effects of word length and visual contrast in the fusiform and lingual gyri during reading. *Proc R Soc Lond B Biol Sci* **267**:1909–13.

Narr KL, Toga AW, Szeszko P, *et al.* (2005) Cortical thinning in cingulate and occipital cortices in first episode schizophrenia. *Biol Psychiatry* **58**:32–40.

Oertel-Knochel V, Knochel C, Rotarska-Jagiela A, *et al.* (2013) Association between psychotic symptoms and cortical thickness reduction across the schizophrenia spectrum. *Cereb Cortex* **23**:61–70.

Olabi B, Ellison-Wright I, McIntosh AM, *et al.* (2011) Are there progressive brain changes in schizophrenia? A meta-analysis of structural magnetic resonance imaging studies. *Biol Psychiatry* **70**:88–96.

Owen MJ, Sawa A, Mortensen PB (2016) Schizophrenia. *Lancet* **388**:86–97.

Palejwala AH, Dadario NB, Young IM, *et al.* (2021) Anatomy and white matter connections of the lingual gyrus and cuneus. *World Neurosurg* **151**:e426-e437.

Pan Y, Pu W, Chen X, *et al.* (2020) Morphological profiling of schizophrenia: cluster analysis of MRI-based cortical thickness data. *Schizophr Bull* **46**:623–32.

Reavis EA, Lee J, Wynn JK, *et al.* (2017) Cortical thickness of functionally defined visual areas in schizophrenia and bipolar disorder. *Cereb Cortex* **27**:2984–93.

Rimol LM, Nesvag R, Hagler DJ, Jr., *et al.* (2012) Cortical volume, surface area, and thickness in schizophrenia and bipolar disorder. *Biol Psychiatry* **71**:552–60.

Shen X, Finn ES, Scheinost D, *et al.* (2017) Using connectome-based predictive modeling to predict individual behavior from brain connectivity. *Nat Protoc* **12**:506–18.

Stephan-Otto C, Siddi S, Cuevas Esteban J, *et al.* (2016) Neural activity during object perception in schizophrenia patients is associated with illness duration and affective symptoms. *Schizophr Res* **175**:27–34.

Suzuki M, Kasai K, Mizuno M, *et al.* (2020) T22. Relationship between cortical thickness and functional outcome in individuals at risk of psychosis. *Schizophr Bull* **46**: S239–40.

Usui N, Haji T, Maruyama M, *et al.* (2009) Cortical areas related to performance of WAIS Digit Symbol Test: a functional imaging study. *Neurosci Lett* **463**:1–5.

van Erp TGM, Walton E, Hibar DP, *et al.* (2018) Cortical brain abnormalities in 4474 individuals with schizophrenia and 5098 control subjects via the Enhancing Neuro Imaging Genetics Through Meta Analysis (ENIGMA) Consortium. *Biol Psychiatry* **84**:644–54.

van Haren NE, Schnack HG, Cahn W, *et al.* (2011) Changes in cortical thickness during the course of illness in schizophrenia. *Arch Gen Psychiatry* **68**:871–80.

Vita A, De Peri L, Deste G, *et al.* (2015) The effect of antipsychotic treatment on cortical gray matter changes in schizophrenia: does the class matter? A meta-analysis and meta-regression of longitudinal magnetic resonance imaging studies. *Biol Psychiatry* **78**:403–12.

Voineskos AN, Jacobs GR, Ameis SH (2020) Neuroimaging heterogeneity in psychosis: neurobiological underpinnings and opportunities for prognostic and therapeutic innovation. *Biol Psychiatry* **88**:95–102.

Wang LJ, Huang YC, Hung CF, *et al.* (2017) The Chinese version of the Brief Assessment of Cognition in Schizophrenia: data of a large-scale Mandarin-speaking population. *Arch Clin Neuropsychol* **32**:289–96.

Wang LJ, Lin PY, Lee Y, *et al.* (2016) Validation of the Chinese version of Brief Assessment of Cognition in Schizophrenia. *Neuropsychiatr Dis Treat* **12**:2819–26.

Xiao Y, Liao W, Long Z, *et al.* (2021) Subtyping schizophrenia patients based on patterns of structural brain alterations. *Schizophr Bull* sbab110.

Xiao Y, Lui S, Deng W, *et al.* (2015) Altered cortical thickness related to clinical severity but not the untreated disease duration in schizophrenia. *Schizophr Bull* **41**:201–10.

Zhang W, Deng W, Yao L, *et al.* (2015) Brain structural abnormalities in a group of never-medicated patients with long-term schizophrenia. *Am J Psychiatry* **172**:995–1003.